ELSEVIER

Biochimica et Biophysica Acta 1564 (2002) 99–106

BIOCHIMICA ET BIOPHYSICA ACTA
BBA

www.bba-direct.com

# Asp$^{344}$ and Thr$^{345}$ are critical for cation exchange mediated by NhaD, $Na^+/H^+$ antiporter of *Vibrio cholerae*

Elena Ostroumov, Judith Dzioba, Peter C. Loewen, Pavel Dibrov *

*Faculty of Science, Department of Microbiology, University of Manitoba, R3T 2N2 Winnipeg, Manitoba, Canada*

Received 4 December 2001; received in revised form 25 March 2002; accepted 27 March 2002

**Abstract**

The Vc-NhaD is an $Na^+/H^+$ antiporter from *Vibrio cholerae* belonging to a new family of bacterial $Na^+/H^+$ antiporters, the NhaD family. In the present work we mutagenized five conserved Asp and Glu residues and one conserved Thr residue to Ala in order to identify amino acids that are critical for the antiport activity. All mutations fall into two distinct groups: (i) four variants, Glu$^{100}$Ala, Glu$^{251}$Ala, Glu$^{342}$Ala, and Asp$^{393}$Ala, did not abolish antiport activity but shifted the pH optimum to more alkaline pH, and (ii) variants Asp$^{344}$Ala, Asp$^{344}$Asn, and Thr$^{345}$Ala caused a complete loss of both $Na^+/H^+$ and $Li^+/H^+$ antiport activity whereas the Asp$^{344}$Glu variant exhibited reduced $Na^+/H^+$ and $Li^+/H^+$ antiport activity. This is the first mutational analysis of the antiporter of NhaD type and the first demonstration of Thr residue being indispensable for $Na^+/H^+$ antiport. We discuss the possible role of Asp$^{344}$ and Thr$^{345}$ in the functioning of Vc-NhaD. 

*Keywords:* $Na^+/H^+$ antiport; *Vibrio cholerae*; Site-directed mutagenesis; Cation-binding site

## 1. Introduction

Bacterial sodium proton antiporters are ubiquitous secondary ion transporters playing important roles in cellular ion homeostasis. They expel toxic $Na^+$ and $Li^+$ ions from the cytoplasm at the expense of the proton motive force (pmf) generated by primary proton pumps, thereby linking $H^+$ and $Na^+$ circulation across the membrane. These proteins are key elements in bacterial membrane energetics, pH homeostasis, and halotolerance (see Refs. [1–3] for review). Enterobacteria typically have a pair of specific $Na^+$ ($Li^+$)/$H^+$ antiporters, NhaA [4] and NhaB [5]. The biochemical properties of the NhaA and NhaB from *Escherichia coli* have been extensively studied in the laboratory of Dr. E. Padan [6–12]. Both proteins exchange more than one proton per sodium ion [6–9]. The activity of Ec-NhaB is pH-independent whereas that of Ec-NhaA increases dramatically upon pH shift from 7.0 to 8.0 [8]. Functional NhaA forms homooligomers (most probably, dimers) in the membrane of *E. coli* [13].

Despite this large body of data, surprisingly little is known about the molecular mechanism that tightly couples cation and proton exchange in $Na^+/H^+$ antiporters. Ec-NhaA remains the only bacterial $Na^+/H^+$ antiporter, which has been the subject of a systematic mutational analysis to identify amino acid residues involved in cation binding and transfer. Three Asp residues, D133, D163, and D164, located within TMS IV and TMS V of the Ec-NhaA, are critical for antiporter activity, presumably providing liganding groups for transported alkali cations [14,15]. These residues are conserved in the NhaA family, and in phylogenetically more distant antiporters from various yeast species [16] including *Schizosaccharomyces pombe*, where the residues are essential for function [17]. Therefore, while intramembrane acidic residues in NhaA-like antiporters are indispensable for the antiport activity [16], residues critical for function in other groups of bacterial $Na^+/H^+$ antiporters remain unknown.

Recently, we cloned a new $Na^+/H^+$ antiporter from *Vibrio cholerae*, Vc-NhaD, [18] which is present in the *V. cholerae* membrane in addition to NhaA and NhaB [18,21]. Six conserved polar residues of Vc-NhaD are identified in this report and variants in these residues are constructed to study their role in the cation–proton exchange.

* Corresponding author. Tel.: +1-204-474-8059; fax: +1-204-474-7603.
*E-mail address:* dibrovp@ms.umanitoba.ca (P. Dibrov).

0005-2736/02/$ - see front matter 
PII: S0005-2736(02)00407-8

## 2. Materials and methods

### 2.1. Materials

All chemicals were from Fisher Scientific or Sigma Chemical Co. Restriction nucleases were from Gibco-BRL, MBI Fermentas or New England Biolabs. The Transformer Site-directed Mutagenesis Kit was purchased from Clontech.

### 2.2. Bacterial strains and culture conditions

The $Na^+/H^+$ antiporter-deficient (*mel*BLid, ΔNhaB1, *cam*$^R$, ΔNhaA1, *kan*$^R$, Δ*lac*ZY, *thr*1) strain of *E. coli*, EP432 was kindly provided by Dr. E. Padan (Hebrew University of Jerusalem, Israel). For routine cloning and plasmid construction, DH5α (US Biochemical Corp.) was used as host. The *mutS E. coli* BMH 71-18 (Clontech) was used to propagate mutated double-stranded DNA. *V. cholerae* strain 0395-N1 was kindly donated by Dr. J. Mekalanos (Harvard Medical School). If not indicated otherwise, cells were grown in modified L broth (LBK) in which NaCl was replaced by KCl [6]. For growth experiments, LBK medium was used in which the starting pH was adjusted between 4.5 and 8.5 by the addition of sterile Hepes–HCl (pH 4.5 to 7.0) or Tris–HCl (pH 7.7 to 8.5) to the final concentration of 20 mM prior inoculation of cells. All media were supplemented with 100 μg/ml ampicillin. Cells were inoculated at $OD_{600} = 0.05$ and grown aerobically at 37 °C for 7 h. Resulting growth was measured as the optical density of bacterial suspension at 600 nm and plotted as a function of starting pH for the control (LBK without additions), LBK supplemented with 0.3 M NaCl or LBK supplemented with 0.1 M LiCl (Fig. 2).

### 2.3. Site-directed mutagenesis

Site-directed mutagenesis of residues Glu$^{100}$, Glu$^{251}$, Glu$^{342}$, Asp$^{344}$, Thr$^{345}$, and Asp$^{393}$ of Vc-NhaD was performed with the Transformer Site-directed Mutagenesis Kit (Clontech) as recommended by the manufacturer. The commercial *Sca*I/*Stu*I trans oligo (Clontech) was used as a selection primer to obtain all mutations. The mutagenic oligonucleotide primers (described in Table 1) were designed to create or remove specific restriction enzyme sites (listed in Table 1). As a template for mutagenesis, the plasmid pBLDL (pBluescript II KS+(Stratagene) containing the *nhaD* gene together with the 300-bp-long 5′ and 230-bp-long 3′ flanking sequences as a 1837-bp *Eco*RI–*Bam*HI insert) was used [18]. Mutated plasmid DNA was isolated from selected transformant clones and digested by the following enzymes to excise the minimal *nhaD* fragments containing the target mutation. *Bcl*I and *Eco*RI were used to obtain a 536-bp fragment with the E100A mutation. *Bcl*I and *Nco*I were used to obtain a 558-bp fragment with the E251A mutation. *Bam*HI and *Nco*I were used to obtain a 723-bp fragment with E342A, D344N, D344A, T345A, and D344E mutations. Mutated fragments were then used to replace the respective sequences in the original (nonmutated) pBLDL. Fidelity of all final mutated versions of *nhaD* in pBLDL was verified by DNA sequencing.

### 2.4. Isolation of membrane vesicles and assay of $Na^+/H^+$ antiport activity

Inside-out membrane vesicles were obtained by passing a bacterial suspension through a French press (Aminco) and assayed for $Na^+/H^+$ antiport activity as described previously [18,22]. Protein content in membrane vesicles was determined by the Bio-Rad Detergent Compatible Protein Assay Kit. The $Na^+/H^+$ antiporter activity was registered by the acridine orange fluorescence dequenching. Aliquots of vesicles (300 μg of protein) were resuspended in 2 ml of a medium containing 100 mM KCl, 250 mM sucrose, 10 mM $MgSO_4$, 0.5 μM acridine orange, and 50 mM Hepes–Tris buffer adjusted to the indicated pH. Respiration-dependent formation of the ΔpH was initiated by the addition of 10 mM Tris–D-lactate, and the resulting quenching of acridine orange fluorescence was monitored with the Shimadzu RF-1501 spectrofluorophotometer (excitation at

Table I
Mutagenic primers used for site-directed mutagenesis in NhaD

| Mutation | Mutagenic primer[a] | Codon → change | Restriction site added (+) or removed (−) |
|---|---|---|---|
| E100A | CTTGAATACGCAG**C**GCTGCTGCTGTTTTTATTGGTCGCC | GAG → GCG | +*Hha*I |
| E251A | CCAGCATCCAAGAAGTGGTCG**C**GCTTAAACGCGA | GAG → GCG | +*Hha*I |
| E342A | GCATTTCTCACGCCG**CC**TGGGACACTTTACTGTTTTTCTATGGGG | GAA → GCC | +*Eco*RII |
| D344N | GCATTTCTCACGCCGAATGG**A**ACAC**G**TTACTGTTTTTCTATGGGG | GAC → AAC | +*Afl*III |
| D344A | CGCCGAATGGG**C**CACTTTACTGTTTTTC | GAC → GCC | −*Bsm*FI |
| D344E | CGCCGAATGGGA**A**ACTTTACTGTTTTTC | GAC → GAA | −*Bsm*FI |
| D393N | GGCTGCTTTCTTCGGTGGTC**AA**C**C**AACAATCCTGTC | GAT → AAC | +*Hin*cII |
| D393A | CGGTGGTCG**CG**AACATTCCTGTC | GAT → GCG | +*Bsp*68I |
| D393E | CGGTGGTCGA**A**AACATTCCTGTC | GAT → GAA | +*Xmn*I |
| T345A | GCCGAATGGGAC**G**CTTTACTGTTTTTTC | ACT → GCT | +*Hga*I |

[a] The mutated nucleotides are shown in boldface.

492 nm and emission at 528 nm). $Na^+/H^+$ antiporter activity was estimated based on its ability to dissipate the established ΔpH upon addition of indicated concentrations of NaCl or LiCl (10 mM in the pH-profile determination; 0.5 to 20 mM for the determination of half-maximal effective concentration). The antiport activities are expressed as percent restoration of the lactate-induced fluorescence quenching.

### *2.5. Addition of 6×His tag to the C-terminus of Vc-NhaD and N-terminal sequencing of tagged protein*

To add the 6 × His tag to the C-terminus of Vc-NhaD, the PCR reaction was carried out using pBLDL as a template. The forward PCR primer was 5′-act aaa cat ATG ACG GGC CGG ATC GCA CTA C-3′ (adds *Nde*I restriction site, underlined), and the reverse PCR primer was 5′-att tga gtc gac

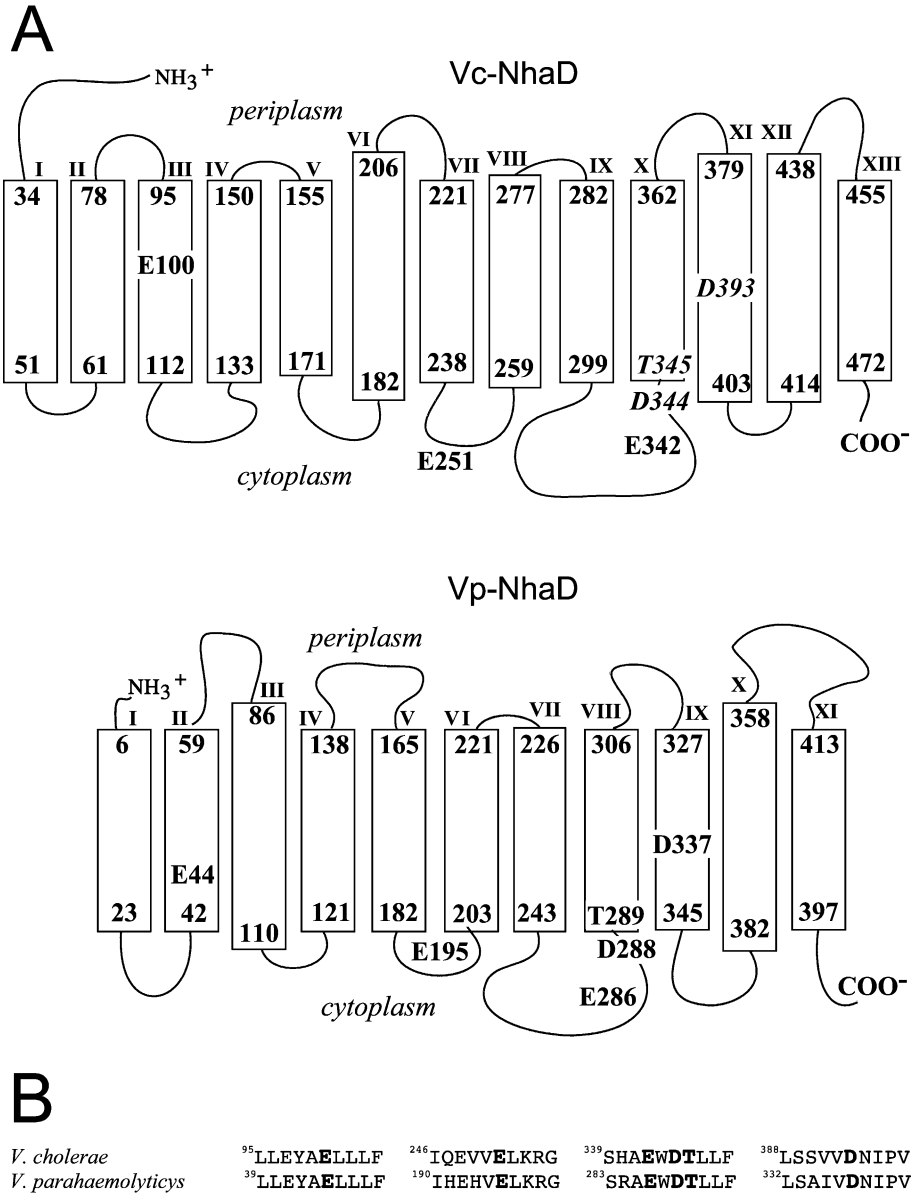


Fig. 1. Conserved polar residues in Vc-NhaD selected for mutagenesis. Panel A: Putative membrane topology of NhaD from *V. cholerae* and *V. parahaemolyticus*. The model was constructed using the HMMTOP program [26]. Residues selected for mutagenesis in Vc-NhaD and their analogs in Vp-NhaD are shown. Residues affecting the ion exchange in Vc-NhaD are given in italics. Panel B: Partial alignments of the derived amino acid sequence of NhaD from *V. cholerae* and NhaD from *V. parahaemolyticus*. Alignments are shown for five negatively charged acidic residues (E100, E251, E342, D344, and D393) whose topology is presumably conserved in both antiporters. Threonine at the position 296 is "topologically" conserved as well. Residues chosen for mutagenesis are given in boldface; numbers preceding sequences indicate the number of the first amino acid.

TGT GAA TGA TTG ATG ATT GAG C-3′(adds *Sal*I site, underlined). The PCR product was cloned into the pET22b+ vector (Novagen), yielding pETL construct. The C-terminal part of the constructed (tagged) Vc-NhaD is: VDKLAAALEHHHHHH. The pETL was digested with *Esp*I, treated with Klenow fragment to produce blunt ends, and digested with *Stu*I. The terminal portion of *nhaD* with added tag was cloned into pBLDL digested with *Stu*I and *Ecl*136I, yielding plasmid pBDH, which contained *nhaD*–6 × His downstream of its natural promoter. Validity of the resulting pBDH construct was confirmed by sequencing.

EP432 cells were electroporated with pBDH, and membrane vesicles were isolated as described above from 4 l of late-logarithmic culture grown on LBK supplemented with 0.1 M LiCl. Isolated membranes were washed once and resuspended in 3 ml of Buffer A containing 60 mM choline–Cl, 100 mM sucrose, 20% glycerol, 20 mM MOPS, pH 7.0; 10 mM imidazole, PMSF and 10 mM β-MEt. Membranes were solubilized by addition of 1% dodecyl β-D-maltoside (DDM) and incubation for 45 min at 23 °C. Solubilized protein was bound to $Ni^{2+}$–NTA resin (Qiagen) in a batch at 23 °C for another 45 min, washed three times with Buffer A containing 0.1% DDM, 20 mM imidazole, and 700 mM NaCl, and eluted into 0.3 ml of the same buffer containing 300 mM imidazole and 1 M NaCl. Eluate was precipitated by TCA, re-dissolved in SDS PAGE loading buffer, and subjected to the SDS PAGE in 10% polyacrylamide gel. After the electrotransfer onto Immobilon-P membrane, a major protein band migrating with an apparent molecular mass close to 54 kDa (calculated molecular mass of tagged Vc-NhaD is 54.109 kDa) was excised from the membrane, dried, and used for the direct N-terminal sequencing (performed in the Protein Microsequencing Laboratory at University of Victoria, British Columbia).

### 2.6. Sequence alignments and NhaD topological model

A screen of genomic databases was carried out using the TBLASTIN program [20]. It confirmed the presence of highly homologous NhaD-like genes in pathogenic *Vibrio parahaemolyticus* [19] and *V. cholerae* [21]. Their partial alignments showing the conserved polar residues located within or associated with putative transmembrane segments are given in Fig. 1A. Putative membrane topology model of NhaD from *V. cholerae* (Fig. 1B) was constructed based on the Topopredict II [25] and HMMTOP [26] programs.

## 3. Results

### 3.1. Determination of the translational start of the Vc-NhaD gene

Comparison of the derived amino acid sequences of NhaD from *V. cholerae* and *V. parahaemolyticus* reveals an interesting feature of Vc-NhaD. The first 49 residues of Vc-NhaD have no homologues in Vp-NhaD, but starting from Met-50 of Vc-NhaD, both proteins show very high degree of homology (78% identity and 88% similarity when aligned by BLASTP 2.0.9 program). We therefore decided to determine the actual N-terminal sequence of functional Vc-NhaD. This information is important for the topology modeling and the selection of target amino acid residues for site-directed mutagenesis (see the next section). To purify Vc-NhaD, a 6 histidine tag was added to the C-terminus of Vc-NhaD as described in Materials and methods. The resulting plasmid, pBDH, containing the *nhaD* gene encoding the protein with additional 15 amino acids, $^{478}$V-D-K-L-A-A-A-L-E-H-H-H-H-H-H$^{492}$, was introduced into the $Na^+/H^+$ antiporter-deficient *E. coli* strain, EP432. Similarly to the EP432/pBLDL transformants (harboring wild-type variant of NhaD), transformant cells of EP432/pBDH, but not parental EP432 cells, were able to grow in LBK medium in the presence of 0.1 M LiCl (data not shown). Inside-out membrane vesicles of EP432/pBDH demonstrated both $Na^+/H^+$ and $Li^+/H^+$ antiport activity (not shown), further confirming both proper targeting and active functional state of the tagged antiporter. We were able to purify tagged Vc-NhaD expressed from its own promoter in a single step using the $Ni^{2+}$ chelation chromatography to produce a major band with an apparent molecular mass of 54 kDa (data not shown). Since the calculated molecular mass of tagged Vc-NhaD is 54,109 Da if the protein starts with Met-1 rather than Met-50, the electrophoretical mobility indicated that mature protein expressed in *E. coli* contained an additional N-terminal segment absent in Vp-NhaD. This was further confirmed by the results of direct N-terminal sequencing of tagged Vc-NhaD, which gave the $^{1}$M-T-G-R-I-A-L-L-S-L-T-L-F$^{13}$ sequence for the first 13 amino acids of the protein.

### 3.2. Selection of targets for site-directed mutagenesis

Acidic amino acid residues located within or associated with transmembrane segments (TMSs) of antiporter proteins are natural candidates for the binding and transfer of alkali cations, which, if replaced by an aliphatic groups, will inactivate the antiport. In the absence of experimental data about membrane topology, the only way of predicting the putative TMSs is computer modeling, and a probable membrane topology of Vc-NhaD derived using the HMMTOP program [26] is shown in Fig. 1A. Another popular program, Topopredict II [25], yielded a very similar model. According to the model, Vc-NhaD has 13 TMSs, varying from 17 to 24 residues in length. Application of the HMMTOP program to Vp-NhaD resulted in a model with 11 TMSs. Combining topological models of Vc-NhaD and Vp-NhaD with their sequence alignment, one can identify negative residues that are located within or near the putative transmembrane segments. Only two intramembrane acidic residues, E100 and D393, are con-

served in both Vp-NhaD and Vc-NhaD (Fig. 1B). However, TMS IX of Vc-NhaD has the conserved polar T345 preceded by the conserved acidic D344, which is located at the membrane–cytoplasm interface (Fig. 1A), a peculiar "border" location that is conserved in both antiporters. In both cases, another conserved acidic residue (E342 in the case of Vc-NhaD) is located in a long cytoplasmic loop close to the DT-harboring TMS (Fig. 1A,B). The position of E97 in Vc-NhaD is ambivalent: it belongs to the TMS III in Vc-NhaD, but its counterpart in Vp-NhaD is located at the membrane–cytoplasm interface. Similarly, D154 of Vc-NhaD is at the membrane–periplasm interface of the TMS V in Vc-NhaD, but its analog (D98) in Vp-NhaD is located in the middle of the putative TMS III. In this work, we restrict our analysis to residues which are predicted to have the same location in both antiporters: E100 and D393 (intramembrane), D344-T345 pair (membrane–cytoplasm interface), E342 (cytoplasm, near DT pair). For the control, E251 has been chosen (presumably located in the middle of a cytoplasmic loop in both proteins). All these residues were replaced by alanine to study their role in the antiport.

### *3.3. Effect of $Glu^{100}$Ala, $Glu^{251}$Ala, $Glu^{342}$Ala, $Asp^{344}$Ala, $Asp^{393}$Ala, and $Thr^{345}$Ala mutations on bacterial growth*

The Vc-NhaD variants were expressed in EP432, the $Na^+/H^+$ antiporter-deficient strain of *E. coli*, to assess their effect on growth (Fig. 2). The pBLDL plasmid used for transformation [18] allowed the expression of the wild-type or mutated antiporter from natural *nhaD* promoter. Being devoid of "domestic" $Na^+/H^+$ antiporters, EP432 cells are highly sensitive to both $Na^+$ and $Li^+$ ions (Fig. 2A), and transformation of EP432 with the wild-type Vc-NhaD restored the ability to grow in the presence of 0.3 M NaCl and 0.1 M LiCl over the pH range 4.5 to 8.0 (Fig. 2B). $Glu^{100}$Ala, $Glu^{251}$Ala, $Glu^{342}$Ala, and $Asp^{393}$Ala variants also supported growth of EP432 transformants in the presence of $Na^+$ or $Li^+$ ($Asp^{393}$Ala is shown in Fig. 2C as an example). By contrast, the $Asp^{344}$Ala and $Thr^{345}$Ala variants did not support growth ($Thr^{345}$Ala is shown in Fig. 2D as an example). Thus, only mutation of $Asp^{344}$ and of its closest neighbor, $Thr^{345}$, altered the Vc-NhaD activity sufficiently to affect the resistance of EP432 transformants to sodium and lithium.

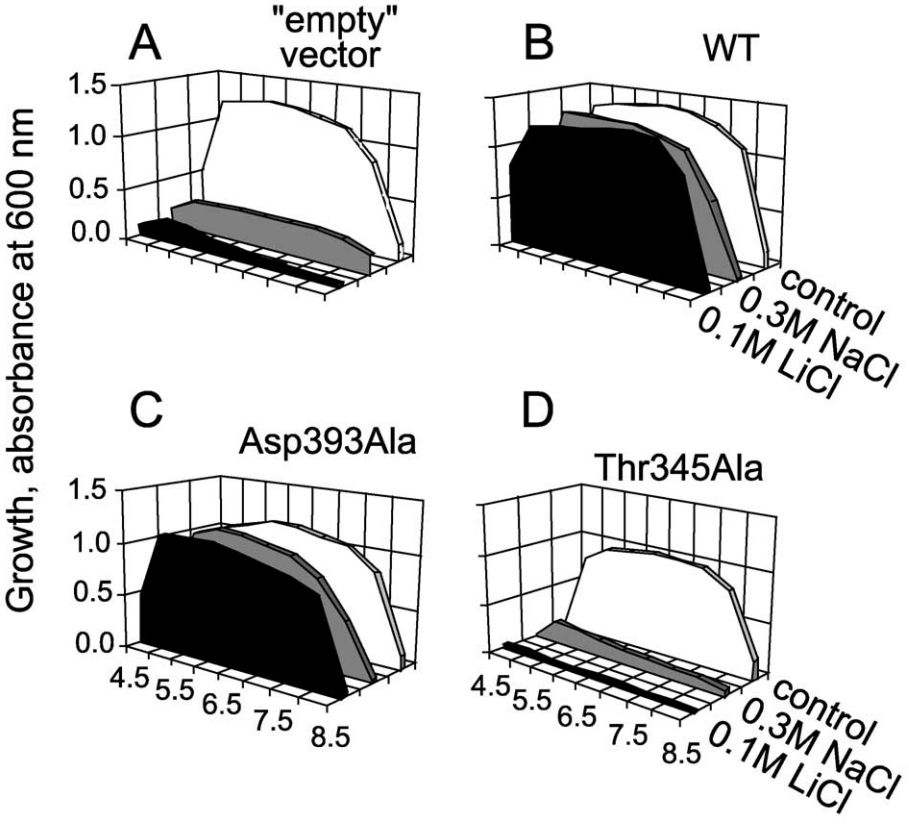


Fig. 2. Effect of mutations on the growth of EP432 transformants. Aerobic growth for 7 h in different media was assessed as described in the text. Panel A: Negative control. EP432 cells were transformed with "empty" pBluescript vector. Panel B: EP432 cells transformed with pBLDL plasmid encoding nonmutated Vc-NhaD. Panel C: EP432 cells transformed with the $Asp^{393}$Ala Vc-NhaD. Substitutions $Glu^{100}$Ala, $Glu^{251}$Ala, and $Glu^{342}$Ala gave similar results (not shown). Panel D: EP432 cells transformed with the $Thr^{345}$Ala Vc-NhaD. The $Asp^{344}$Ala mutant had similar growth properties (data not shown).

### 3.4. Asp[344]Ala and Thr[345]Ala mutations result in inactivation of the cation/proton antiport

To characterize the effect of Asp[344]Ala and Thr[345]Ala variants on the activity of NhaD directly, we measured $Na^+/H^+$ and $Li^+/H^+$ antiport activities in inside-out membrane vesicles prepared from corresponding EP432 transformants.

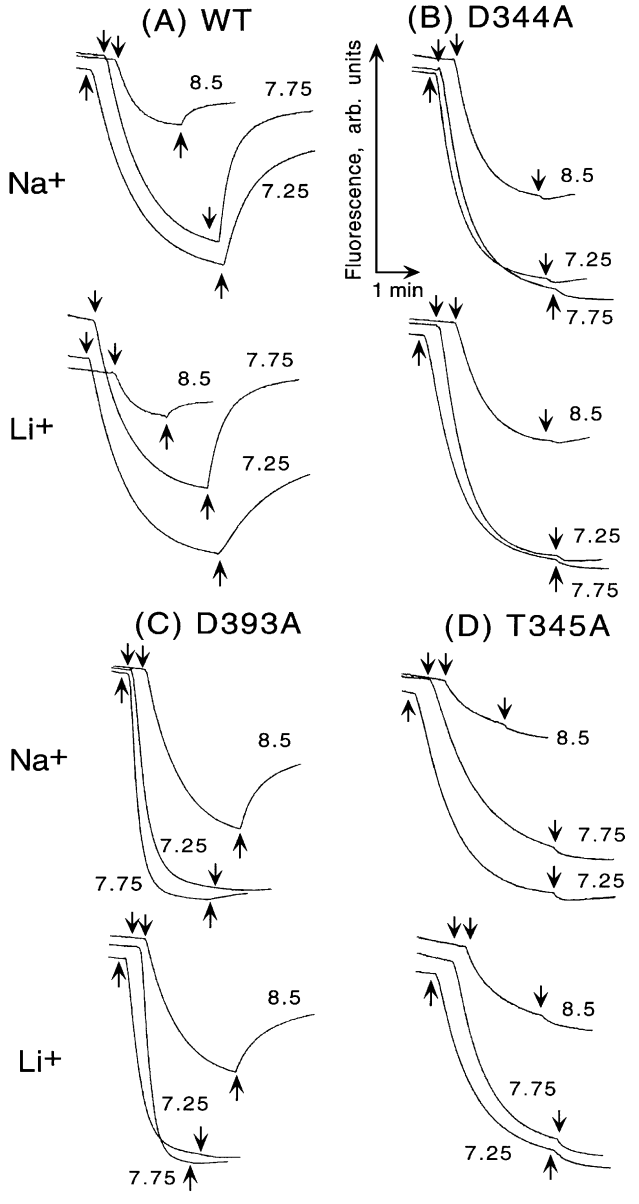


Fig. 3. $Na^+/H^+$ and $Li^+/H^+$ antiport activities in the inside-out membrane vesicles from Vc-NhaD mutants. Membrane vesicles were prepared from EP432 cells carrying the wild-type (A, positive control) or a mutant (B–D) *nha*D expression plasmid, and assayed as described in Materials and methods. Data shown represent typical result of one of at least three independent experiments. First arrow at each trek indicates the addition of lactate. Second arrow indicates the addition of 10 mM NaCl or LiCl. The upper and bottom panels show $Na^+/H^+$ and $Li^+/H^+$ antiport activity, respectively. pH of the experimental mixture is given at each trek. See text for further details.

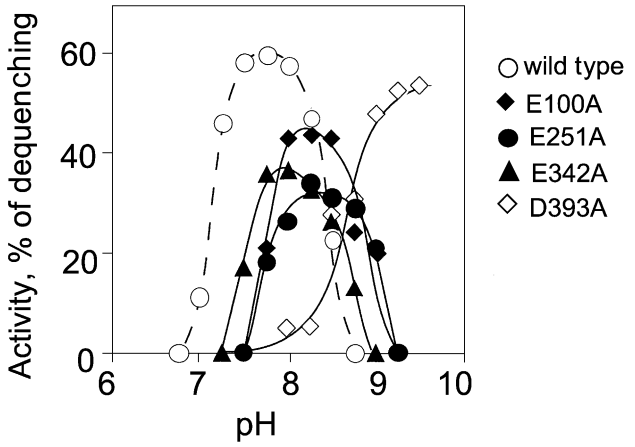


Fig. 4. pH profiles of $Na^+/H^+$ antiport activity in Vc-NhaD mutants. Activities were measured as in previous figure and expressed as percent restoration of the lactate-induced fluorescence quenching. Each point represents an average of two independent measurements. pH profiles of $Li^+/H^+$ antiport in each mutant were nearly identical to those of $Na^+/H^+$ antiport (not shown).

Addition of 10 mM NaCl or LiCl to vesicles prepared from EP432 cells transformed with wild-type Vc-NhaD led to partial dissipation of respiration-induced ΔpH at pH 7.25, 7.75, and 8.5 due to the cation/proton antiport. By contrast, membranes containing Asp[344]Ala and Thr[345]Ala variants of NhaD showed no $Na^+/H^+$ or $Li^+/H^+$ antiport activity at any pH tested (Fig. 3B,D). The Asp[393]Ala variant of NhaD was active at pH 8.5, however at pH 7.75 the activity was barely detectable (Fig. 3C), indicating a shift in the pH-profile of its activity toward more alkaline pH.

Indeed, pH-profiles of the activity of Glu[100]Ala, Glu[251]Ala, Glu[342]Ala, and Asp[393]Ala variants (Fig. 4) revealed activities slightly lower than the wild type and shifted toward alkaline pHs by 0.25–0.5 pH unit. Variant Asp[393]Ala has the distinctive property of a pH profile shifted by more than 1.5 pH units toward alkaline pH (Fig. 4). This variant was most active at pH 9.5. At pH higher than 9.5, vesicles showed rather weak response on the addition of respiratory substrates, impeding quantitation of the antiport activity. In any of these four mutants, the pH-profiles of $Li^+/H^+$ and $Na^+/H^+$ antiport activity were nearly identical as is the case for wild-type antiporter (data not shown). Therefore, these mutations do not change the cation selectivity of Vc-NhaD, and the observed changes in pH-profiles of activity do not abolish the ability of the Vc-NhaD variants to support the growth of EP432 transformants in the presence of $Na^+$ and $Li^+$ ions (even in the Asp[393]Ala mutant, see Fig. 2C).

### 3.5. Further examination of Asp[344] and Asp[393] residues

Asp[344] and Asp[393] residues were chosen for further study, largely because of the results just described. Asp[393] was also chosen because of its apparent analogy with Asp[133]

of Ec-NhaA, where intramembrane Asp rather than Glu residues were indispensable for activity [3,14,15]. Indeed, the $Asp^{133}$Ala variant of Ec-NhaA was partially active [15] much like $Asp^{393}$Ala in Vc-NhaD, while the $Asp^{133}$Asn variant showed no cation/proton antiport activity [14]. In addition, the $Asp^{393}$Ala variant of Vc-NhaD resulted in the largest shift of the pH profile of activity (Fig. 4), implying the prominent influence of this residue on the activity. Replacement of $Asp^{344}$ with Glu resulted in a partially active protein (Fig. 5B) whereas the $Asp^{344}$Asn mutation inactivated the antiport (Fig. 5A), confirming the importance of the negatively charged side chain. As in Ec-NhaA, the $Asp^{393}$Asn variant of Vc-NhaD was unable to catalyze the cation/proton antiport (Fig. 5C), as was the $Asp^{393}$Glu variant (Fig. 5D).

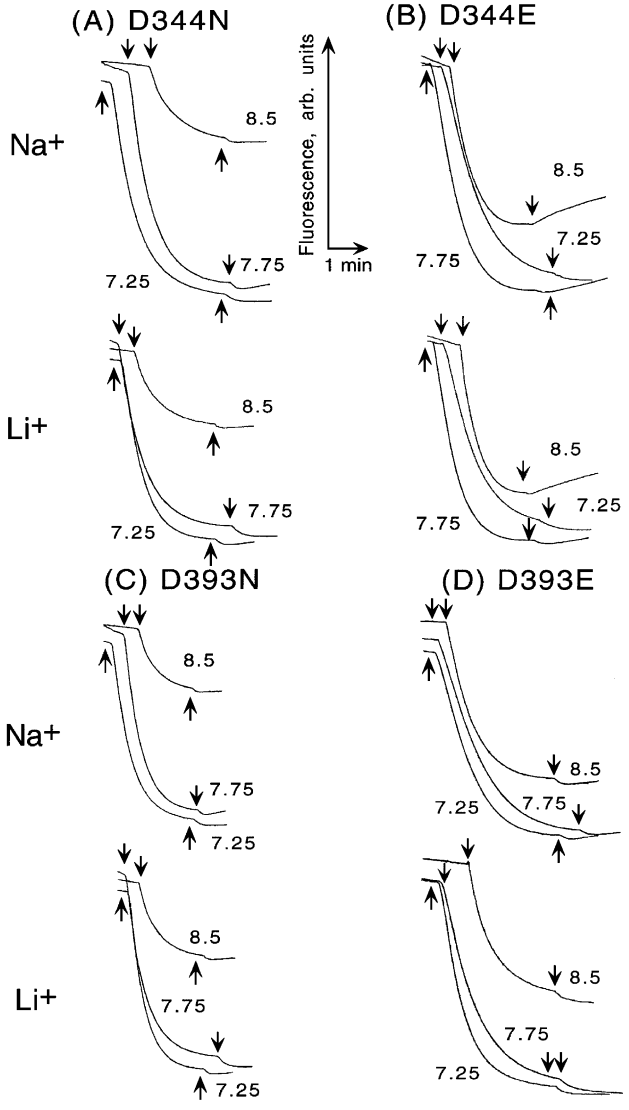


Fig. 5. $Na^+/H^+$ and $Li^+/H^+$ antiport in the membrane vesicles from $Asp^{344}$Asn, $Asp^{344}$Glu, $Asp^{393}$Asn, and $Asp^{393}$Glu mutants; all experimental conditions as in Fig. 3. Note that only $Asp^{344}$Glu mutant showed measurable antiport activities.

## 4. Discussion

The major finding of this work is that the two conserved adjacent polar residues, $Asp^{344}$ and $Thr^{345}$, are critical for the function of Vc-NhaD with both Ala substitutions abolishing antiport (Fig. 3B,D). Replacement of $Asp^{344}$ by Asn led to the same effect (Fig. 5A). In contrast, introduction of another acidic residue, Glu, instead of $Asp^{344}$ yielded partially active antiporter (Fig. 5B). Therefore, a carboxyl group in the position 344 and hydroxyl in the position 345 seem to be mandatory for function. In both bacterial [3,14,15,27] and yeast [16,17] $Na^+/H^+$ antiporters, conserved intramembrane Asp residues have been found to be essential for activity, presumably forming the cation-binding site [14,15]. However, the involvement of $Thr^{345}$ in the case of Vc-NhaD is intriguing. To the best of our knowledge, this is the first example of Thr residue being indispensable for $Na^+/H^+$ antiport. Our mutagenesis was already completed when Galili et al. [28] reported that the mutation of the Ec-NhaA $Thr^{132}$ (adjacent to the functionally significant $Asp^{133}$) into Cys does not abolish the cation–proton exchange completely but dramatically changes the apparent $K_m$ of the antiporter. The authors mutagenized $Thr^{132}$ based on the analogy with bacterial $Na^+$-ATPase where neighboring acidic and hydroxyl-containing residues are believed to form the cation-binding site [24]. Indeed, it is very tempting to speculate that the putative cation-binding site of Vc-NhaD may be formed by $Asp^{344}$ and $Thr^{345}$ in a manner similar to the subunit c of the $Na^+(Li^+,H^+)$–motive ATPase of *P. modestum*, where the pair of adjacent residues with carboxyl and hydroxyl groups is clearly involved in the binding of translocated cations [23,24]. However, it should be stressed here that the measurements of fluorescence dequenching give information about the entire catalytic cycle of the antiporter but not about its partial reactions such as recognition/binding of alkaline cations, their translocation, and coupling to the oppositely directed proton movement. Therefore, it is not clear at the moment whether $Asp^{344}$ and $Thr^{345}$ of Vc-NhaD are directly involved in alkali cation binding or are essential for the conformational changes occurring during other steps of the catalytic cycle, e.g., cation translocation.

Our mutational analysis of Vc-NhaD revealed that four of five conserved acidic amino acid residues, which are presumably associated with transmembrane segments, are dispensable for antiporter activity. Mutations $Glu^{100}$Ala, $Glu^{251}$Ala, $Glu^{342}$Ala, and $Asp^{393}$Ala did not either arrest the activity of the antiporter or change the cation specificity but did shift its pH-profile toward more alkaline pH (Fig. 4). Since the $Asp^{393}$Ala variant retains some activity (Fig. 3C), $Asp^{393}$ obviously is not indispensable for function, in contrast to $Asp^{344}$ or $Thr^{345}$. However, the $Asp^{393}$Asn and $Asp^{393}$Glu variants are unable to catalyze cation/proton antiport (Fig. 5C,D). This, to some extent, resembles the $Asp^{133}$ residue in Ec-NhaA [3,14,15]. In both antiporters, mutation of the corresponding Asp into Asn (but not into Ala) abolishes $Na^+/H^+$ antiport completely. It is noteworthy

that although the $Asp^{393}$Ala variant showed no significant activity at pH below 8.0 when assayed in inside-out vesicles (Fig. 4), it nevertheless supported growth in the presence of $Na^+$ or $Li^+$ at much lower external pH (Fig. 2C). The most probable reason for such apparent discrepancy is that the activity of the $Asp^{393}$Ala variant below pH 8.0 is too low to be measured in vesicles in the fluorescence dequenching assay, but is sufficient for supporting growth. The similar situation was recently reported and the same explanation suggested for the A127V variant of Ec-NhaD, which supports the growth of the EP432 transformants in the presence of $Na^+$ at pH 8.3 but shows no measurable activity when assayed in everted membrane vesicles at this pH [28].

Further experiments are needed to elucidate mechanism of $Na^+/H^+$ exchange catalyzed by Vc-NhaD. Detailed in-depth analysis, including the measurement of downhill $Na^+$ transport and counterflow experiments, is required to clarify the role of $Asp^{344}$, $Thr^{345}$ and $Asp^{393}$. It should be mentioned also that the topological model of Vc-NhaD presented here (Fig. 1A) still is a hypothetical one. We plan to examine the topological structure of Vc-NhaD and its mechanistic aspects in our future works.

## Acknowledgements

This work was supported by the Operating Grant no. 34021 from the Manitoba Health Research Council and by the Operating Grant no. 227414-00 from the Natural Sciences and Engineering Research Council of Canada (to EO, JD, and PD) and by a grant no. RGP9600 from the Natural Sciences and Engineering Research Council of Canada (to PCL).

## References

[1] E. Padan, S. Schuldiner, in: E. Bakker (Ed.), Alkali Cation Transport Systems in Procaryotes, CRC Press, Boca Raton, FL, 1992, pp. 3–24.
[2] E. Padan, S. Schuldiner, Biochim. Biophys. Acta 1185 (1994) 129–151.
[3] E. Padan, M. Venturi, Y. Gerchman, N. Dover, Biochim. Biophys. Acta 1505 (2001) 144–157.
[4] B.G. Goldberg, T. Arbel, J. Chen, R. Karpel, G.A. Mackie, S. Schuldiner, E. Padan, Proc. Natl. Acad. Sci. U. S. A. 84 (1987) 2615–2619.
[5] E. Pinner, E. Padan, S. Schuldiner, J. Biol. Chem. 267 (1992) 11064–11068.
[6] E. Padan, N. Maisler, D. Taglicht, R. Karpel, S. Schuldiner, J. Biol. Chem. 264 (1989) 20297–20302.
[7] E. Pinner, Y. Kotler, E. Padan, S. Schuldiner, J. Biol. Chem. 268 (1993) 1729–1734.
[8] D. Taglicht, E. Padan, S. Schuldiner, J. Biol. Chem. 266 (1991) 11289–11294.
[9] E. Pinner, E. Padan, S. Schuldiner, J. Biol. Chem. 269 (1994) 26274–26279.
[10] D. Taglicht, E. Padan, S. Schuldiner, J. Biol. Chem. 268 (1993) 5382–5387.
[11] P. Dibrov, D. Taglicht, FEBS Lett. 336 (1993) 525–529.
[12] P. Dibrov, FEBS Lett. 336 (1993) 530–534.
[13] Y. Gerchman, A. Rimon, M. Venturi, E. Padan, Biochemistry 40 (2001) 3403–3412.
[14] H. Inoue, T. Noumi, T. Tsuchiya, H. Kanazawa, FEBS Lett. 363 (1995) 264–268.
[15] T. Noumi, H. Inoue, T. Sakurai, T. Tsuchiya, H. Kanazawa, J. Biochem. 121 (1997) 661–670.
[16] P. Dibrov, L. Fliegel, FEBS Lett. 424 (1998) 1–5.
[17] P. Dibrov, P.G. Young, L. Fliegel, Biochemistry 37 (1998) 8282–8288.
[18] J. Dzioba, E. Ostroumov, A. Winogrodzki, P. Dibrov, Mol. Cell. Biochem. 229 (2002) 119–126.
[19] K. Nozaki, T. Kuroda, T. Mizushima, T. Tsuchiya, Biochim. Biophys. Acta 1369 (1998) 213–220.
[20] S. Altschul, T. Madden, A. Schaffer, J. Zhang, Z. Zheng, W. Miller, D. Lipman, Nucleic Acids Res. 25 (1997) 3389–3402.
[21] C.C. Häse, N.D. Fedorova, M.Y. Galperin, P. Dibrov, Microbiol. Mol. Biol. Rev. 65 (2001) 353–370.
[22] M. Harel-Bronstein, P. Dibrov, Y. Olami, E. Pinner, S. Schuldiner, E. Padan, J. Biol. Chem. 270 (1995) 3816–3822.
[23] Y. Zhang, R.H. Fillingame, J. Biol. Chem. 270 (1995) 87–93.
[24] G. Kaim, F. Wehrle, U. Gerike, P. Dimroth, Biochemistry 36 (1997) 9185–9194.
[25] M. Claros, G. von Heijne, Comput. Appl. Biosci. 10 (1994) 685–686.
[26] G.E. Tusnády, I. Simon, J. Mol. Biol. 283 (1998) 489–506.
[27] T. Nakamura, Y. Komano, T. Unemoto, Biochim. Biophys. Acta 1230 (1995) 170–176.
[28] L. Galili, A. Rothman, L. Kozachkov, A. Rimon, E. Padan, Biochemistry 41 (2002) 609–617.